ELSEVIER

Journal of Power Sources 70 (1998) 48–54

JOURNAL OF POWER SOURCES

Characterization of commercially available lithium-ion batteries

Bradley A. Johnson, Ralph E. White *

Center for Electrochemical Engineering, Department of Chemical Engineering, University of South Carolina, Columbia, SC 29208, USA

Received 19 December 1996; revised 11 March 1997

Abstract

With the aggressive growth of the lithium-ion battery market, several companies have recently offered their version of the lithium-ion battery for consumer purchase. This paper describes the physical design, rate, cycle-lifetime, and self-discharge performance of cells from Sony, Matsushita, A&T, Moli, and Sanyo lithium-ion batteries. The study used a total of 85 lithium-ion cells from these manufacturers. All cells performed as indicated by manufacturers' specifications and the performance and design differences are discussed. The design differences include discussion of gas chromatography–mass spectroscopy (GC–MS) analysis of the electrolytes, a differential scanning calorimetry (DSC) analysis of separators, the activation of a positive temperature coefficient (PTC), and a comparison of the basic physical parameters of each cell. Performance characterization shows an excellent high discharge rate performance of the A&T and Matsushita cells, an excellent cycle-lifetime performance for Sony cells, and negligible effects of self-discharge. © 1998 Elsevier Science S.A.

Keywords: Lithium-ion batteries; Batteries; Electrolytes; Separators; Rate; Cycle-life performance ; Self-discharge

1. Introduction

The lithium-ion battery market has been in a period of dynamic growth ever since Sony introduced the first commercial cell in 1991 [1]. With energy densities exceeding 130 Wh/kg and cycle-lifetimes of more than 1000 cycles, the lithium-ion battery system has become increasingly popular in applications such as portable computers, camcorders, and cellular phones. As more lithium-ion battery manufacturers enter the market and new materials are developed, cost reduction should only spur growth in new applications. Yoda [2] has considered this advancement and described a future battery society in which the lithium-ion battery plays a dominant role. Although the Sony system has been characterized before [3], this paper will examine the differences in design, performance, and materials used in cells from current lithium-ion battery manufacturers.

Although no manufacturer was willing to supply the study with cells due to the liability involved, a total of 85 cells produced by five different manufacturers were obtained. The cells were taken from cellular phone packs, portable computer packs, and camera packs purchased both in the USA and Japan. The manufacturers represented include Sony, Sanyo Electric, Matsushita Electric Industrial, Moli Energy, and A&T Battery. All cells were the 18 650 size, except the Matsushita cells, which were the 17 500 size. Although Matsushita lists the 18 650 size in their literature, none could be located for this study. The 18 650, which is 18 mm in diameter and 65.0 mm tall, was considered to be a standard cell to reference as it is the most commonly used cell.

2. Cell construction analysis

The primary objective of the cell construction analysis was to examine the differences in cell designs for the different manufacturers. The secondary objective was to analyze the individual components of the cell for direct comparison. To achieve these objectives, one to two uncycled cells from each manufacturer was dissected and analyzed. Prior to dissection, each cell was fully discharged in order to reduce the risks associated with accidental short-circuit of the cell during dissection. For further precaution, the cell was dissected in a dry room (dew point approximately −40 °C). Each can was opened by carefully cutting a small slit in the top of the can and peeling back the

* Corresponding author. Tel.: +1-803-777 32 70; fax: +1-803-777 82 65; e-mail: rew@engr.sc.edu

0378-7753/98/$19.00 © 1998 Elsevier Science S.A. All rights reserved.
PII S0378-7753(97)02659-1

RJ Technology Exhibit 2009
Apple Inc. v. RJ Technology LLC
IPR2023-01350, Page 1 of 8

crimped portion of the can which encompasses the header. During this process, a majority of the electrolyte evaporated such that a quantitative analysis of the electrolyte was impossible. This evaporation was quite evident as a sweet odor was present from the moment the slit was cut in the top of the can, except for the A&T cell. Once the can was peeled away, the header could then be removed by severing the positive tab. A metal tube with outside diameter of 3.9 mm was removed from the center of the A&T electrode roll. The tube had a slit that ran lengthwise in which the negative tab could be inserted and spot welded to the bottom of the can. The electrode roll was removed from the can once the negative tab had been freed from this spot weld. A plastic disk with a small hole in the center was located at the bottom of each can. In each case, the negative tab had joined the can through this center hole. The plastic disk insulated the cathode edges from shorting out on the can. There was no electrolyte present in the bottom of any can.

The electrode rolls were wrapped tightly and were held together with a piece of tape on the outside seam. As shown in Fig. 1, each electrode roll had a layer of separator on the outside, followed by the anode, another layer of separator and the cathode on the inside. Immediately after opening the roll, electrolyte was collected from the electrodes by dropping isopropyl alcohol (IPA) onto the electrode surface and letting it drip into a collection bottle. This procedure was performed over the length of both electrodes such that the final volume of IPA and electrolyte collected was 10–20 ml. Table 1 shows the results of the gas chromatography–mass spectroscopy (GC–MS) analysis of these samples. As expected, propylene carbonate was the primary component of the Sony system, which uses a coke-based anode, while ethylene carbonate was the primary component of the other systems, which have graphite-based anodes. Although quantitative analysis was not possible, actual electrolyte and salt ratios were likely at the point of maximum conductivity for the given mixtures [4–6].

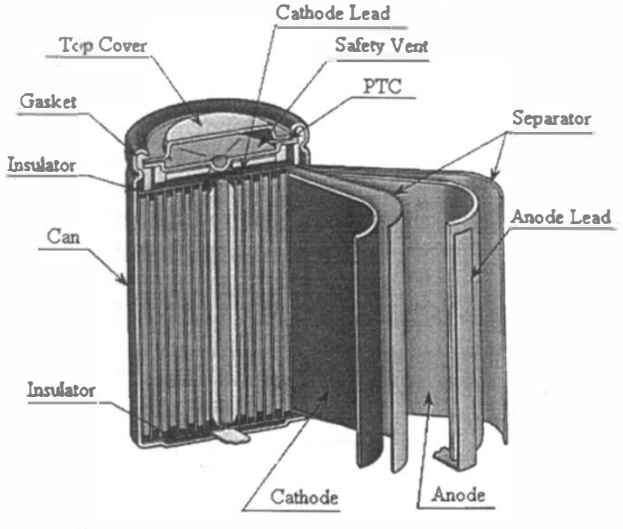


Fig. 1. Cutaway view of a typical lithium-ion battery.

Table 1
GC–MS analysis of electrolytes

Manufacturer	Components
Sony	PC, DMC, MEC
Moli	EC, DEC
A&T	EC, MEC
Sanyo	EC, DMC, DEC
Matsushita	EC [a], DMC, DEC, MEC
Key	EC = ethylene carbonate
	PC = propylene carbonate
	DMC = dimethyl carbonate
	DEC = diethyl carbonate
	MEC = methyl ethyl carbonate

[a] Note: Although no EC was detected, Matsushita claims to use an EC-based electrolyte [7]

Differential scanning calorimetry (DSC) was performed on the separators from each cell and the results are shown in Table 2. All separators were either polyethylene (PE) or polypropylene (PP). PE separators are used as secondary safety mechanisms which help to limit cell temperatures by melting, which closes pores, stops mass transfer between electrodes, and thereby increases cell resistance. High temperatures may occur during runaway reactions induced by short-circuit or overcharge. The PP separators have too high of a melt temperature to work in this way because either venting or mechanical disconnect will generally occur first [8]. Only Moli did not use a PE separator, while the Sony cell actually used one PE separator and one PP separator. This does not imply that Sony used a two-ply separator or that two separators were sandwiched together. In the Sony case, a PP separator was used on one side of each electrode, while a PE separator was used on the other side. In this case, it is possible that shutting down half of the cell is sufficient to stop a runaway reaction while the other half of the cell effectively discharges itself. Besides material differences, the separators had important physical differences, which indicated that they were produced by a variety of manufacturers. The A&T and Sanyo separators were very soft, had a tendency to wrinkle, and were stretched easily in one direction. The PP Sony and Moli separators were very smooth to the touch and stretched easily in one direction as well, while the PE Sony and

Table 2
DSC analysis of separators

Manufacturer	Melt temperature (°C)	Components
Sony Separator 1 [a]	161.7	Polypropylene
Sony Separator 2 [a]	134.2	Polyethylene
Moli	163.6	Polypropylene
A&T	135.8	Polyethylene
Sanyo	135.4	Polyethylene
Matsushita	133.9	Polyethylene

[a] Note: This does not imply the use of a two-ply separator. See text.

RJ Technology Exhibit 2009
Apple Inc. v. RJ Technology LLC
IPR2023-01350, Page 2 of 8

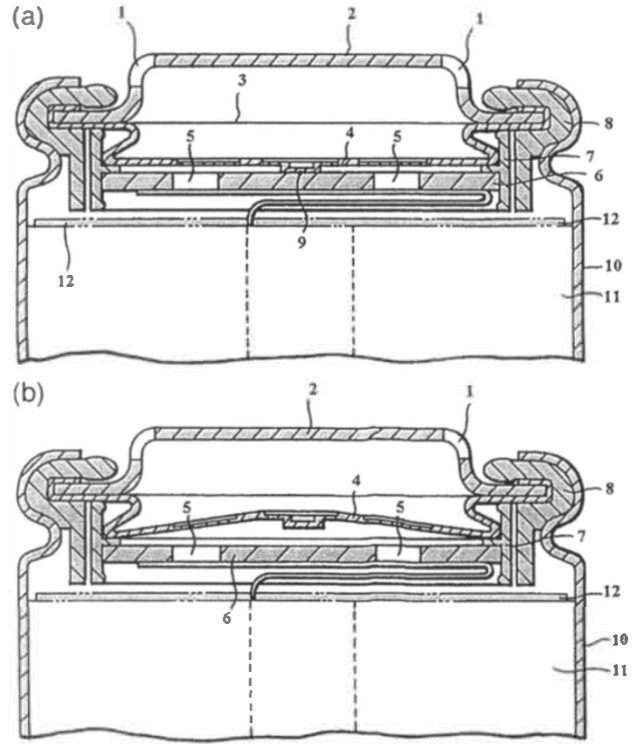


Fig. 2. (a) Schematic diagram of a Sony lithium-ion cell header assembly in its normal mode of operation. (b) Schematic diagram of a Sony lithium-ion header assembly after the current disconnect mechanism has been utilized.

Matsushita separators were smooth to the touch and had high tensile strengths in both directions.

The header was the one component that varied a great deal in design between each manufacturer. Fig. 2(a) and (b) gives schematic diagrams of a Sony header [9]. The main components of the header include: (1) vented; (2) positive button/lid; (3) positive temperature coefficient (PTC); (4) aluminum burst disk; (5) vented; (6) metal disk; (7) plastic ring, and (8) plastic sheath. At its center, a small (9) tip protruded and was spot welded to a (6) metal disk. The metal disk and the burst disk were separated by a (7) plastic ring that encompassed the metal disk and held it some distance from the burst disk. This distance was bridged by the length of the protruding tip. Pressure build-up within the cell would force the safety valve upward thereby disconnecting the current, as shown in Fig. 2(b). Under extreme pressure, the burst disk should break and thereby release pressure. A (8) plastic sheath encased the components of the header and insulated it from the (10) can. For the Moli and Matsushita cells, this casing served the dual purpose of insulating the header from the (11) electrode roll. Sony and Sanyo had a separate (12) plastic disk similar to the one in the bottom of the can to serve this purpose. The A&T header was by far the most complex design. Instead of a (12) plastic disk, A&T incorporated a highly machined 0.3 g, 38 mil thick component that resembled circuit board material. In addition, the A&T design did not have a circuit disconnect as described earlier. Their header featured an extremely malleable burst disk and PTC. Overall, it contained two more components than any of the other designs. These steel disks weighed 0.78 g and their function was unclear. Headers from other manufacturers were similar in concept to the Sony header as described, but differed in the actual design.

A primary safety device found in all cells was the PTC. Its function is to stop the current flow if the cell overheats. It is constructed of two steel disks separated by a layer composed of carbon and a proprietary conductive polymer. Upon overheating, the carbon/polymer layer, which is normally a dense crystalline structure, expands and creates a non-conductive amorphous structure between the steel disks. Furthermore, the expansion is reversible if the load is removed and the PTC is allowed to cool sufficiently. Fig. 3 demonstrates this process. In the figure, a current of 12 A was applied to the Matsushita PTC. As the temperature neared 70 °C, the carbon/polymer structure expanded, thus stopping current flow through the PTC and the device started cooling. The initial temperature was well above ambient temperature because the reversibility of the expansion had been tested several times. PTCs from other cells were not tested.

The electrode components were measured and weighed, with the results shown in Table 3. The mass of the active materials was determined by taking the mass of the electrode minus the mass of the tab and current collector, which was estimated by using the thickness, length, width, and density of the current collector material. All manufacturers used Li_xCoO_2 cathode materials [7,10–13], while either graphite or coke-based anode materials were used, as described later. For all cases, the negative electrode used a 0.7 mil thick copper current collector, while the positive electrode used a 1.0 mil thick aluminum current collector. All electrode thicknesses shown are the average of five measurements at various points along the length of the given electrode. These measurements were performed with a L.S. Starrett No. 1230 micrometer. The total length and width represent the dimensions of the current collector, while the area of active material accounts for the geometric surface area of the given current collector that was covered. There were several key differences between the cells. The most significant difference was that the A&T cell only had active material on one side of its

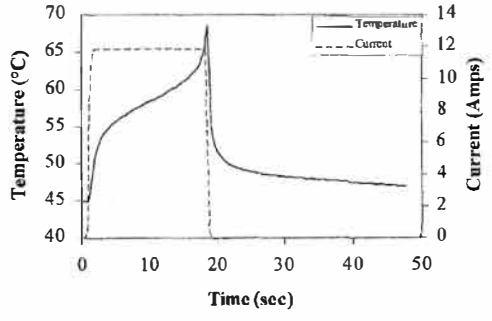


Fig. 3. Performance of the Matsushita PTC with a 12 A applied current.

RJ Technology Exhibit 2009
Apple Inc. v. RJ Technology LLC
IPR2023-01350, Page 3 of 8

Table 3
Physical parameters of commercial lithium-ion cells

		Sony	Moli	A&T	Sanyo	Matsushita
	Total cell mass (g)	39.4	41.9	40.8	38.1	24.1
	Mass of can (g)	9.1	9.0	7.6	6.6	4.5
	Mass of header (g)	1.3	1.1	2.1	1.2	1.1
Positive	Total electrode mass (g)	15.5	14.4	13.6	13.3	7.0
	Total length (cm)	52.1	49.2	78.1	49.5	35.0
	Total width (cm)	5.3	5.5	5.4	5.4	3.7
	Total thickness (μm)	185	178	114	180	185
	Foil thickness (μm)	25	25	25	25	25
	Geometric area of active material (cm^2)	493	532	422	498	254
	Mass of active material (g)	13.6	12.5	10.6	11.3	6.2
Negative	Total electrode mass (g)	9.1	12.0	9.4	10.2	7.5
	Total length (cm)	53.3	53.3	76.8	51.9	42.2
	Total width (cm)	5.6	5.7	5.5	5.6	3.9
	Total thickness (μm)	193	203	94	163	216
	Foil thickness (μm)	18	18	18	18	18
	Geometric area of active material (cm^2)	542	603	421	577	308
	Mass of active material (g)	3.5	6.9	2.5	6.4	4.7
Separator	Mass (g)	1.7	1.3	2.2	2.0	1.6
	Length (cm)	118.1	109.6	173.4	117.4	101.6
	Width (cm)	5.9	5.9	5.3	5.6	4.4
	Thickness (μm)	25	25	25	25	25

current collectors, while all other cells had active material on both sides of the current collectors. This design appears to have an excessive current collector mass; however, A&T has made up for this with a high capacity graphite, which is described later. Another significant difference between the cells is the large difference in can masses. It was difficult to measure the can's thicknesses due to its curvature; however, all cans appeared to be identical, except for their mass. Anode active material surface areas exceeded those of cathode active material surface areas by 10 to 20% in all cases but one, as the A&T active material surface areas were matched evenly. For the A&T cell, with only one side of the current collector covered, electrode fabrication and battery assembly may have been a simpler task even though there would be a small capacity increase with double-sided electrodes, as a smaller fraction of the volume and mass of the cell would be occupied by the current collector. By taking ratios of positive to negative active material masses, one starts to see significant differences between cell designs. Information such as theoretical capacities of electrode materials used by each manufacturer or surface to volume ratios of the materials used would have provided insight towards the performance differences between the manufacturers; however, that information was not available and was not determined.

3. Performance characterization

Performance characterization experiments were performed with a 32 channel Maccor Series 2000 battery tester. For each type of performance characterization, fresh cells were used in order to minimize variations related to capacity decay from cycling. In addition, each performance study used a minimum of three cells from each manufacturer. Furthermore, there was no significant difference between the performance of the cells of each manufacturer. For the cycle-lifetime and self-discharge studies, the noise observed in the data is likely due to the coupled effect of the very long experiment time and the variations in room temperature.

Although the cells had slightly different capacities and different suggested charging protocols, the cells were treated as if they were identical, with exception to the Matsushita cells which were a different size. This allowed a more direct comparison of cells from one manufacturer to another. Therefore, identical charge and discharge procedures were implemented during the study. The most significant variance from some of the manufacturer's suggested cycling criteria was the potential limit used during

Table 4
Charging protocol as specified by manufacturer's product literature

Manufacturer	Current (A)	Potential limit (V)	Time (h)
Sony	1.0	4.2	2.5
A&T	1.0	4.2	2.5
Sanyo	1.3	4.1	2.5
Moli	1.2	4.1	2.5
Matsushita	0.5	4.2	2.0 u

RJ Technology Exhibit 2009
Apple Inc. v. RJ Technology LLC
IPR2023-01350, Page 4 of 8

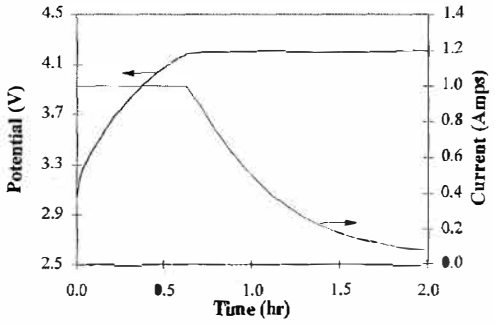


Fig. 4. Characteristics of the charge protocol used for 18650 cells.

cell charging. All manufacturers had suggested potential limits of 4.1 to 4.2 V, while recommended initial currents ranged from 0.5 to 1.3 A and charging times ranged from 2.0 to 2.5 h. The charging protocols specified in each manufacturer's product literature is shown in Table 4. A standard procedure of a 1.0 A charge with a 4.2 V potential limit and 2.0 h charge time was used for the 18650 cells, while a 0.6 A, 4.2 V potential limit, and 2.0 h charge time was used for the Matsushita cells. Since such a small fraction of the capacity is charged during the last half hour of a 2.5 h charge, we used a 2 h charge time to accelerate cycle-life testing and then maintained the same charge protocol for all other performance tests. Fig. 4 shows a typical charge profile using this procedure. Again, this standard was used because of the large capacity difference observed when charging the cells to 4.1 V versus 4.2 V and the importance to have a fair comparison between cells of different manufacturers.

Rate performance testing was performed by discharging the cells at rates ranging from $C/5$ to $3C$. Fig. 5 shows the discharge profiles at these various rates for each manufacturers' cells. The first notable feature is the characteristic shape of the Sony discharge curve. The lack of any potential plateau indicates the use of a coke-based anode material [14]. Without a potential plateau, Sony is sacrificing energy density by using this type of anode material;

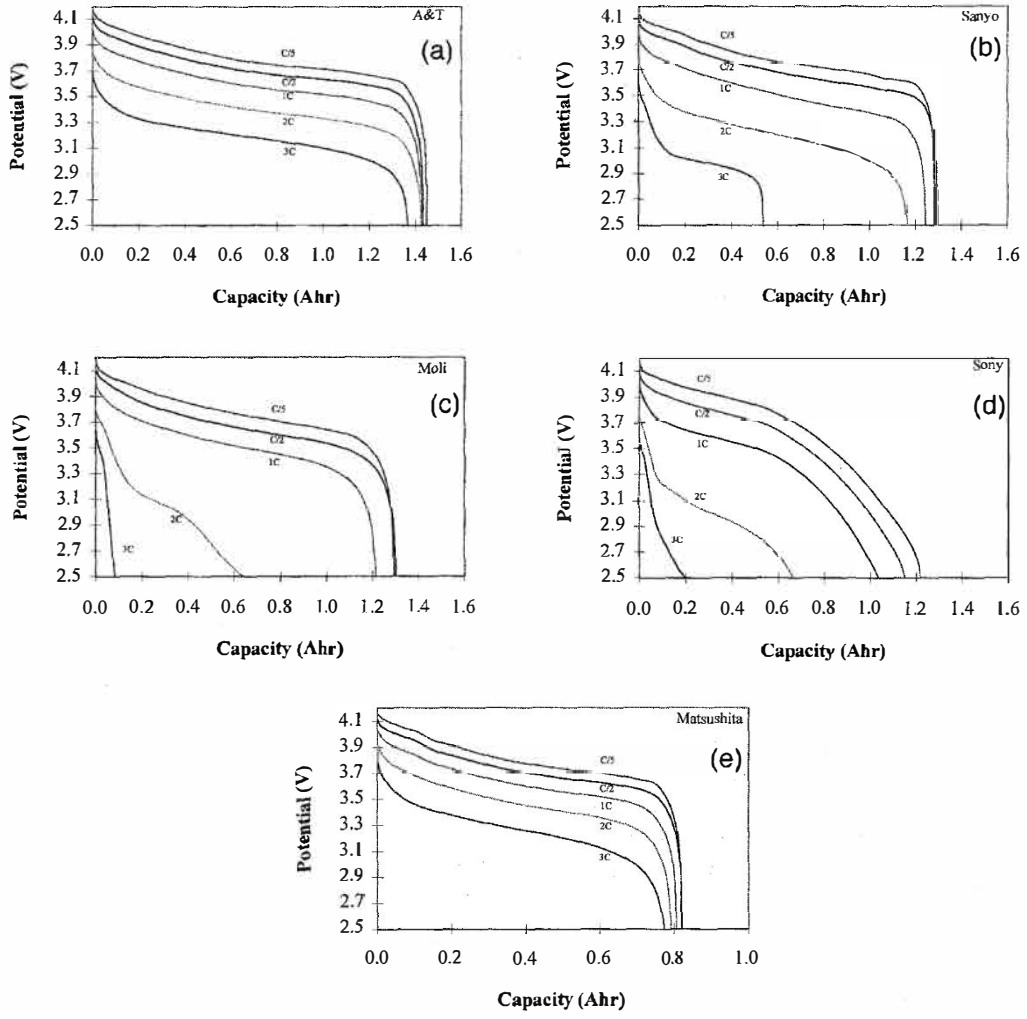


Fig. 5. (a) Discharge comparisons at rates ranging from $C/5$ to $3C$ for the A&T cells. (b) Discharge comparisons at rates ranging from $C/5$ to $3C$ for the Sanyo cells. (c) Discharge comparisons at rates ranging from $C/5$ to $3C$ for the Moli cells. (d) Discharge comparisons at rates ranging from $C/5$ to $3C$ for the Sony cells. (e) Discharge comparisons at rates ranging from $C/5$ to $3C$ for the Matsushita cells.

RJ Technology Exhibit 2009
Apple Inc. v. RJ Technology LLC
IPR2023-01350, Page 5 of 8

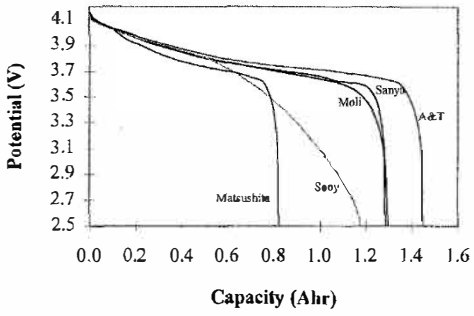


Fig. 6. Comparisons of different manufacturers performance at a $C/5$ discharge rate.

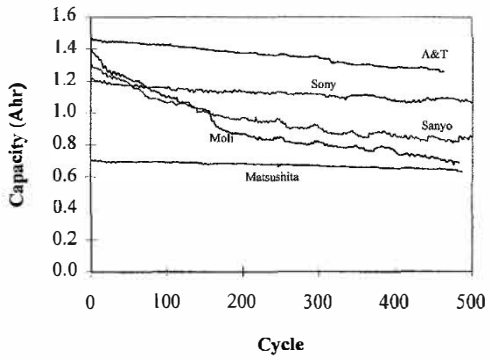


Fig. 7. Cycle-lifetime performance for A&T, Sony, Sanyo, Moli, and Matsushita. All cycles were discharged at a $C/2$ rate.

however, Sony turns this into a positive effect by stating that the potential may be used as a state-of-charge indicator for their system. The disadvantage of having lower energy density is offset by excellent cycle life and a smaller problem associated with electrode swelling during charge/discharge. In addition, the figure shows a large performance discrepancy, especially at high discharge rates. We attribute this to the types, amounts, and specific surface areas of the different carbons used. For example, A&T reported capacity and high discharge rate advantages of using graphitized meso-phase-pitch-based carbon fiber anodes as compared with traditional graphite or coke [15]. The Matsushita cells performed well at the high discharge rates as well. Although most applications do not require such demanding conditions, the versatility of these cells should be noted. However, the performance difference at the high rates is likely observed in an application such as portable computer use. Although the packs generally last in excess of 2 h per charge ($C/2$ discharge rate), it is reasonable to expect current surges during operation. For example, when the portable computer is first switched on, the video display must light simultaneously with a long period of hard drive access. If the use of energy is inefficient during this period, the discharge time observed by the user will be reduced. Fig. 6 summarizes Fig. 5(a)–(e) with a comparison of all cells at the $C/5$ discharge rate. (Note that when accounting for the size of the cell, the Matsushita discharge curve should fall near the A&T curve if it were an 18 650 cell.) The energy densities of the cells at the $C/5$ discharge rate are shown in Table 5. Considering scale-up factors, an 18 650 Matsushita cell would probably have the highest energy density of the cells compared in this study, since a higher proportion of the smaller Matsushita cell is occupied by the can and header.

The cycle-lifetime performance of the cells is shown in Fig. 7. The cells were charged as stated previously and then discharged to 100% depth-of-discharge at a $C/2$ rate. The figure shows that A&T, Sony, and Matsushita have excellent cycle-life performance through 500 cycles, while the capacity of the Moli and Sanyo cells decreased dramatically. The rapid capacity fade rate for the Sanyo and Moli cells is likely due to charging the cells at 4.2 V, even though they were specified to be charged at 4.1 V. However, as previously described, this was done in order to get a fair comparison between cells of different manufacturers for all characterization testing and a significant overall capacity gain was observed when charging at 4.2 V versus 4.1 V. The Sony and Matsushita cells were selected for their excellent performance up to 500 cycles and were then cycled in excess of 1000 cycles. Even after 1000 cycles, the six Sony cells maintained 88% of their initial capacity on average, thus verifying their claim of excellent cycle-life performance with the use of a coke anode. The Matsushita cells saw dramatic decreases in cell capacity between 600–800 cycles. Although time constraints limited the other cycle-lifetime testing to 500 cycles, longer cycle

Table 5
Energy densities at a $C/5$ discharge rate

Cell	Energy density	
	(Wh/kg)	(Wh/l)
Sony US 18650	103	245
A&T LSR 18650	130	321
Sanyo UR 18650	126	288
Moli ICR 18650	113	287
Matsushita CGR 17500	129	269

Table 6
Self-discharge characteristics of the Sony and Matsushita cells

Days	Percent initial capacity (%)	
	Sony US 18650	Matsushita CGR 17500
0	100	100
1	99.0	99.1
5	98.0	99.4
10	96.9	99.1
30	97.5	98.2

RJ Technology Exhibit 2009
Apple Inc. v. RJ Technology LLC
IPR2023-01350, Page 6 of 8

lives would be required in only a few high performance systems. With the average of all manufacturers' cells being 81% of rated capacity at 500 cycles, most of the cells will likely outlive their targeted applications of portable computers, cellular phones, and other miscellaneous electronic devices.

Self-discharge effects of the Sony and Matsushita cells were measured and the results are shown in Table 6. The cells were first cycled five times to insure they fell in the expected capacity range. Then each cell was charged, held at open circuit and ambient temperature (about 25 °C) for a period of time, and discharged. After as long as a 30 day period at open circuit, all cells tested maintained greater than 97% initial capacity and therefore any self-discharge effect was determined to be insignificant.

4. Conclusions

This work shows the large contrast in commercially available lithium-ion batteries. It was evident that the manufacturers have used widely different materials, designs, and safety devices. The most apparent of these differences was the use of a PP separator by Sony and Moli and the lack of a mechanical disconnect in the A&T cells. Several other factors indicated that there is room for cell capacities to increase considerably in the coming years. For example, in A&T's case, small gains could be realized by reducing the volume occupied by their current collectors by using electrodes with active material on both sides. However, larger gains in capacity and energy density are more likely to be realized by developing high capacity carbons. Nevertheless, there are other factors to consider. It was evident that these cells had different strengths. While A&T and Matsushita had excellent rapid discharge characteristics, the Sony cells had outstanding cycle-life characteristics as approximately 90% of initial capacity was observed beyond 1000 cycles. This cycle-lifetime performance was attributed to Sony's use of coke or hard carbons, which do not swell as much during cycling. Although cost, energy density, and safety are currently the predominant concerns, as the lithium-ion battery market matures, there will be new applications that will require good cycle-life performance. With an enormous projected growth of the industry over the next decade, there will certainly be other companies offering new, perhaps better, designs. However, the maintained safety of the lithium-ion battery is critical in achieving these goals.

Acknowledgements

Financial support for this work was provided by National Science Foundation Award GER-9553409, an NSF/EPSCoR Industry Graduate Research Traineeship, and Hoechst Celanese Separation Products. In addition, the authors would like to thank Dr Robert Spotnitz for his useful discussions and laboratory assistance, Dr Sunkwei Huang for analysis of the electrolyte solutions, Mark Ferebee for his laboratory assistance, and Paige Smith for her DSC analysis.

References

[1] O. Kazunori and M. Yokokawa, Cycle performance of lithium ion rechargeable battery, 10th Int. Seminar of Primary and Secondary Battery Technology Applications, 1–4 Mar. 1993, Deerfield Beach, FL, USA, Florida Educational Seminars, Boca Raton, FL.

[2] S. Yoda, Global energy prospects in the 21st century: a battery based society, 8th Int. Meet. Lithium Batteries, 16–21 June 1996, Nagoya, Japan, The Electrochemical Society of Japan.

[3] D. Linden (ed.), Handbook of Batteries, McGraw Hill, New York, 2nd edn., 1995, p. 36.44–48.

[4] M. Ishikawa, M. Morita, M. Asao and Y. Matsuda, J. Electrochem. Soc., 141 (1994) 1105–1108.

[5] M. Terasaki, H. Yoshida, H. Tukamoto, M. Mizutani and M. Yamachi, Denki Kagaku, 61 (1993) 1417–1418.

[6] J.T. Dudley, D.P. Wilkinson, G. Thomas, R. LeVae, S. Woo, H. Blom, C. Horvath, M.W. Juzkow, B. Denis, P. Juric, P. Aghakian and J.R. Dahn, J. Power Sources, 35 (1991) 59–82.

[7] T. Sugimoto, Development of lithium ion rechargeable battery, Power 96, 13–16 Oct. 1996, Santa Clara, CA, USA.

[8] R. Spotnitz, M. Ferebee, R. Callahan, K. Nguyen, W.-C. Yu, M. Geiger, C. Dwiggins, H. Fisher and D. Hoffman, Shutdown battery separators, 12th Int. Seminar of Primary and Secondary Battery Technology and Application, 6–9 Mar. 1995, Deerfield Beach, FL, USA, Florida Educational Seminars, Boca Raton, FL.

[9] K. Taki, K. Togashi, T. Masuko, K. Katayama, T. Yuda, H. Nishikwa and R. Yamane, Eur. Patent Applic. 93 109317.3 (6 Sept. 6 1993).

[10] Molicel ICR-18650 Product Data Sheet, May 1995.

[11] Sony Lithium-Ion Rechargeable Battery Technical Information, Oct. 1995.

[12] A&T Battery Corp. Product Information, undated.

[13] J. Colton, Battery products: technical approaches by worldwide battery manufacturers, Power 96, 13–16 Oct. 1996, Santa Clara, CA, USA.

[14] Y. Nishi, Design and safety challenges of lithium-ion battery product, Power 95, 16–18 Oct. 1995, Santa Clara, CA, BIS Strategic Decisions and Arthur D. Little.

[15] Mo.Kanda, T. Ohsaki, Y. Aoki, H. Shiroki and S. Suzuki, High capacity lithium-ion cells using graphitized mesophase-pitch-based carbon fiber anodes, 8th Int. Meet Lithium Batteries, 16–21 June 1996, Nagoya, Japan, The Electrochemical Society of Japan.

RJ Technology Exhibit 2009
Apple Inc. v. RJ Technology LLC
IPR2023-01350, Page 7 of 8